Reconstructions of toroidal current profiles for bootstrap current discharges in Wendelstein 7-X

John Schmitt[1], T. Andreeva[2], J. Geiger[2], S. Lazerson[2], D. Maurer[1], U. Neuner[2], N. Pablant[3], K. Rahbarnia[2], J. Schilling[2], H. Thomsen[2], Y. Turkin[2], and the W7-X Team[2]

[1]Auburn University
[2]Max-Planck-Institut für Plasmaphysik
[3]Princeton Plasma Physics Laboratory

62nd Annual Meeting of the American Physical Society Division of Plasma Physics

November 9 - 13, 2020

Supported by U.S. D.o.E. grant DE-SC00014529

This work has been carried out within the framework of the EUROfusion Consortium and has received funding from the Euratom research and training programme 2014-2018 and 2019-2020 under grant agreement No 633053. The views and opinions expressed herein do not necessarily reflect those of the European Commission.

Outline

Abstract & Background

The reconstruction of the Wendelstein 7-X (W7-X) plasma equilibrium plays an important role in interpreting diagnostic signals and understanding the plasma. The reconstruction is iterative in nature, involving the repeated calculation of the MHD equilibrium and synthetic diagnostic signals and comparing these signals to measured signals. The parameters that describe the equilibrium (shape and location of the plasma boundary and profile information) are adjusted between iterations to find the best-fit of the measured and synthetic signals. These profiles are then used to interpret diagnostic information and for further physics analysis.
The predicted evolution of the current profile is compared to the reconstructions constrained by magnetic diagnostics, Thomson Scattering, interferometry, x-ray imaging crystal spectroscopy, and boundary conditions based on the proximity to the 5/5-island chain. The time-evolved current density profile, based on transport simulations of toroidal current using NTSS, is compared to reconstructions at several times during the bootstrap discharge. The sensitivity of the reconstruction to the current density profile and its parameterization and dependence on diagnostic constraints and initial profiles will be discussed.

The work here extends the methods presented in

- "Uncertainty Analysis in 3D Equilibrium Reconstruction", M.R. Cianciosa, J.D. Hanson & D.A. Maurer, Fusion Science and Technology, **74** (2018).

Additional background/codes

- **NTSS**: "Neoclassical transport simulations for stellarators", Turkin, Y., Beidler, C. D., Maaßberg, H., Murakami, S., Tribaldos, V., and Wakasa, A., Physics of Plasmas, **18** (2011).
- **VMEC**: "Steepest-descent moment method for three-dimensional magnetohydrodynamic equilibria", Hirshman, S.P. and Whitson, J.C., Phys. Fluids, **26** (1983).
- **V3FIT**: "V3FIT: a code for three-dimensional equilibrium reconstruction" J. D. Hanson, S. P. Hirshman, S. F. Knowlton, L. L. Lao, E. A. Lazarus, and J. M. Shields, Nuclear Fusion, **40** (2009).

V3FIT: An iterative 3-D MHD equilibrium reconstruction

Initial guesses for
1. **Pressure profile**
2. **Current profile**
3. **Enclosed toroidal flux**

Coil set description
Stellarator symmetric
Coil currents are corrected to account for E-M deflections

MHD Calculation
VMEC
Free-boundary
MPOL = 12
NTOR = 12
NTHETA = 36
NZETA = 36
NS = 401
FTOL = 1e-14

Synthetic Diagnostics and Constraints, $S_i^M(\boldsymbol{p})$ and σ_i^S
Magnetic
No diamagnetic or compensation flux loops
Saddle Flux Loops
Rogowski coils (complete)
Rogowski coils (segmented)

Last closed flux surface
Contact with the divertor is a (weighted) target for the position of last closed flux surface

Experimental Data, S_i^O
Magnetic, 5% Arb Uncertainty

Evaluate

$$\chi(\boldsymbol{p})^2 = \sum_i W_i \left(\frac{S_i^O - S_i^M(\boldsymbol{p})}{\sigma_i^S}\right)^2$$

Check
1. $\chi(\boldsymbol{p}) < \chi_{target}$
2. Maximum iteration count reached
3. Some other exit condition reached?

No

Adjust profiles, toroidal flux
Iterative step chosen based on SVD analysis of Jacobian (finite differences).

Yes

Reconstruction complete.
'Best fit' Pressure profile, current profile, and enclosed flux
Post-processing

Reconstruction Variables and Outputs

Inputs & Variables for the V3FIT Reconstruction

Coil Model.	Stellarator Symmetric.
Coil Currents.	Corrected for E-M loading.
Plasma Pressure Profile.	Initial guesses based on Thomson + XICS. Reduced model for reconstruction.
Current profile.	'Sum-of-cos-squared' profiles, 3 regions.
Net toroidal flux.	Targeted (but not constrained) to be touching the divertor.

V3FIT Outputs and Post-Processing

Plasma pressure and current profiles.	'Best-fit' profiles.
Best linear estimates extended to include the pressure and current profiles.	Radial profiles w/ uncertainties.
Net toroidal flux.	Close to, but not necessarily touching the divertor.

A simple model with 2 degrees-of-freedom spans a wide variety of experimentally-inspired pressure profiles

$$P(s) = PRES_{SCALE} \times AM(0) \times \left((1 - AM(3)) \times \left(1 - s^{AM(1)}\right)^{AM(2)} + AM(3) \times \left(1 - s^{AM(4)}\right)^{AM(5)} \right)$$

- 'two_two_power' in VMEC
- Free Parameters
  - $PRES_{SCALE}$
  - $AM(3)$
- Constants
  - $AM(0) = 1.0$
  - $AM(1) = 1.0$
  - $AM(2) = 4.5$
  - $AM(4) = 4.0$
  - $AM(5) = 4.5$

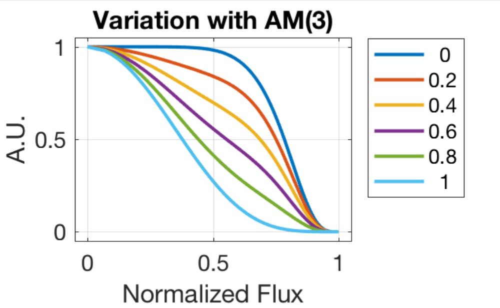

Figure 1: $AM(3)$ is a mixing factor for a linear superposition of two '2-power' profiles.

A radially-'localized' toroidal current density profile with 3-4 free parameters is chosen.

- Toroidal profile shape is specified by an analytic 'sum of cos-squared' profiles with N_{cssq} independent radial 'zones'. In VMEC, $AC(0) = N_{cssq}$
- The profile shape is normalized according to the net toroidal current carried by the plasma. $I(s=1) = CURTOR = \int_{s=0}^{s=1} ds 2\pi J(s)$
- Left: cos^2-basis functions for $N_{cssq} = 3$. The coefficients for $AC(1)...AC(3)$ are used for the blue, red (dashed) and black (dotted) lines, respectively.
- Right: The basis functions are plotted for $N_{cssq} = 4$ and $AC(1)...AC(4)$ would be used for the blue, red, yellow and purple dashed lines, respectively.

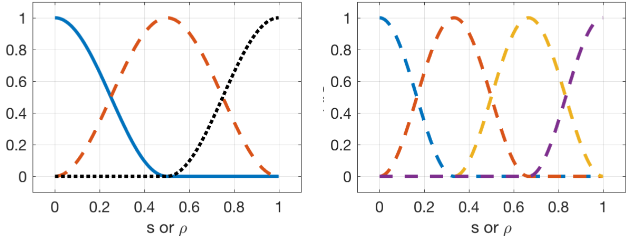

Current profile details

The current profile normalization is determined by the net current, *CURTOR* and a weighted sum of the individual cos^2- coefficients.

- $J(s) = \frac{CURTOR}{2\pi L_1} * L(s)$
- $\Delta x = \frac{1}{(N_{cssq}-1)}$
- $\xi = (i-1) * \Delta x = \frac{(i-1)}{(N_{cssq}-1)}$
- $L_1 = \int_{s=0}^{s=1} dsL(s) = \frac{\frac{AC(1)}{2} + \sum_{i=2}^{N_{cssq}-1} AC(i) + \frac{AC(N_{cssq})}{2}}{N_{cssq}-1}$
- $$L(s) = AC(1)(H(x) - H(x-\Delta x)) * cos^2\left(\pi\frac{(x)}{(2\Delta x)}\right)$$
  $$+ \sum_{k=2}^{N_{cssq}} AC(k)(H(x-(\xi(k)-\Delta x) - H(x-(\xi(k)+\Delta x))*$$
  $$cos^2\left(\pi\frac{(x-\xi(k))}{(2\Delta x)}\right)$$
  $$+AC(N_{cssq})(H(x-1-\Delta x) - H(x-1))*$$
  $$cos^2\left(\pi\frac{(x-1)))}{(2\Delta x)}\right)$$

Uncertainties propagated from the signals to the model and derived parameters based on best linear estimates.

- S_i^O, σ_i: The observed (or measured) values and associated uncertainties
- $S_i^M(\mathbf{p})$: The synthetic model values
- $e_i = \frac{S_i^O - S_i^M(\mathbf{p})}{\sigma_i}$: The 'error' between measurement and synthetic model
- The optimizer minimizes the cost function, $\chi^2 = \sum_i W_i e_i^2$
- $(\mathbf{C_s})_{i,j} = \sigma_i \sigma_j \delta_{ij}$: Signal covariance matrix (uncorrelated)
- $\mathbf{C_p}$: Parameter covariance matrix, $C_p^{-1} = J^T \cdot C_s^{-1} \cdot J$; $J_{i,j} = \frac{\partial e_i}{\partial p_j}$
- $\mathbf{C_M}$: Model-derived covariance matrix, $C_M = K^T \cdot C_p \cdot K$
- The change in the model-derived parameter M_i with respect to changes in the parameter, p_j: $K_{i,j} = \frac{\partial M_i(\mathbf{p})}{\partial p_j}$

The parameter here is the total plasma pressure or toroidal current density at radial index $i \in [1, N_s]$:

- $M_i = J_{tor}((i-1)/(N_s-1))$ or $M_i = P_{total}((i-1)/(N_s-1))$
- $\sigma_{M_i} = \sqrt{\mathbf{C_M(i,i)}}$

The '*two_two_power*' profile and its $K_{i,j}$ terms

$$P(s) = PRES\_SCALE * AM(0) * \left((1 - AM(3)) * \left(1 - s^{AM(1)}\right)^{AM(2)} + AM(3) * \left(1 - s^{AM(4)}\right)^{AM(5)} \right)$$

The elements of $K_{i,j}$ related to the pressure profile are

- $\frac{\delta P(s=i/N_s)}{\delta P_{scale}} = AM(0) \times \left(AM(3) \times \left(1 - s^{AM(1)}\right)^{AM(2)} + (1 - AM(3)) \times \left(1 - s^{AM(4)}\right)^{AM(5)} \right) = \frac{P(s)}{P_{scale}}$
- $\frac{\delta P(s=i/N_s)}{\delta AM(0)} = P_{scale} \times \left(AM(3) \times \left(1 - s^{AM(1)}\right)^{AM(2)} + (1 - AM(3)) \times \left(1 - s^{AM(4)}\right)^{AM(5)} \right) = P(s)/AM(0)$
- $\frac{\delta P(s=i/N_s)}{\delta AM(1)} = -P_{scale} AM(0) AM(2) AM(3) s^{AM(1)} log(s) \left(1 - s^{AM(1)}\right)^{(AM(2)-1)}$
- $\frac{\delta P(s=i/N_s)}{\delta AM(2)} = P_{scale} AM(0) AM(3) log \left(1 - s^{AM(1)}\right) \left(1 - s^{AM(1)}\right)^{AM(2)}$
- $\frac{\delta P(s=i/N_s)}{\delta AM(3)} = P_{scale} AM(0) \times \left(\left(1 - s^{AM(1)}\right)^{AM(2)} - \left(1 - s^{AM(4)}\right)^{AM(5)} \right)$
- $\frac{\delta P(s=i/N_s)}{\delta AM(4)} = -P_{scale} AM(0) (1 - AM(3)) AM(5) s^{AM(4)} log(s) \left(1 - s^{AM(4)}\right)^{(AM(5)-1)}$
- $\frac{\delta P(s=i/N_s)}{\delta AM(5)} = P_{scale} AM(0) (1 - AM(3)) \, log \left(1 - s^{AM(4)}\right) \left(1 - s^{AM(4)}\right)^{AM(5)}$

The elements of $K_{i,j}$ related to the sum-cos^2 current density

The elements of $K_{i,j}$ related to the current density profile are:

- $\frac{\delta J(s=i/N_s)}{\delta(CURTOR)} = \frac{J(s=i/N_s)}{CURTOR}$
- $\frac{\delta J(s=i/N_s)}{\delta(AC(1))} = -\frac{CURTOR*(N_{cssq}-1)}{\left(\sum_{k'=1}^{N_{cssq}} AC(k')\right)^2} * (eqn) + J_{Norm} * 2 * (H(x) - H(x-\Delta x)) * cos^2\left(\pi\frac{(x-\xi(1))}{(2\Delta x}\right)$
- $\frac{\delta J(s=i/N_s)}{\delta AC(k)}\Big|_{k\in 2,N_{cssq}-1} = -\frac{CURTOR*(N_{cssq}-1)}{(\sum_{k'=1}^{N_{cssq}} AC(k'))^2} * (eqn) + J_{Norm} * (H(x - (\xi(k)-\Delta x)) - H(x-(\xi(k)+\Delta x))) * cos^2\left(\pi\frac{(x-\xi(k))}{(2\Delta x)}\right)$
- $\frac{\delta J(s=1)}{\delta AC(N_{cssq})} = -\frac{CURTOR*(N_{cssq}-1)}{(\sum_{k=1}^{N_{cssq}} AC(k))^2} * (eqn) + J_{Norm} * 2 * (H(x - (\xi(N_{cssq})-\Delta x)) - H(x-(\xi(N_{cssq})))) * cos^2(\pi\frac{(x-\xi(N_{cssq}))}{(2\Delta x)})$

Magnetic diagnostics are located behind the heat-shield, close to the plasma.

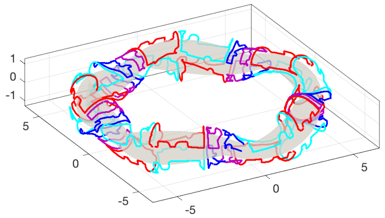

Figure 2: 8 types of saddle coils for each of the 5 field periods (plasma LCFS shown in grey)

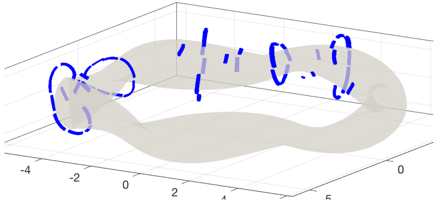

Figure 3: Segmented Rogowski coils provide good poloidal coverage over 2 field periods.

The diamagnetic loops and compensation loops are not used as constraints in the equilibrium reconstructions shown here.

Pressure profile variations with iota, at $t = 3.5$ sec

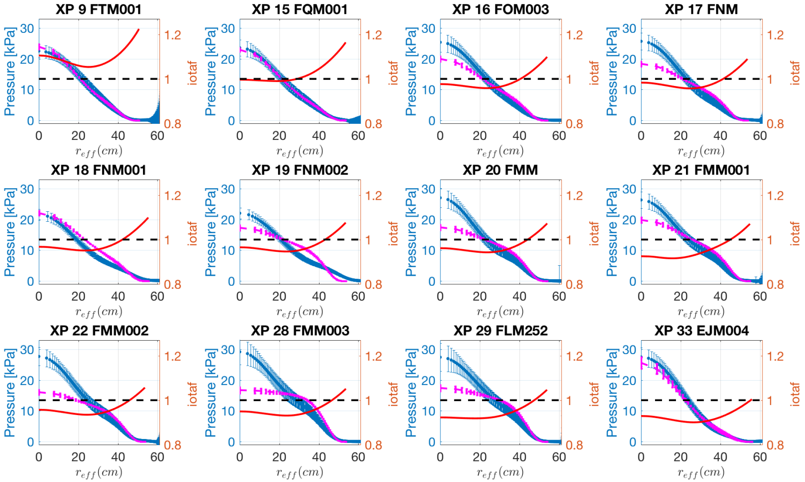

Figure 4: Left axis (Pressure): Kinetic profile data is the basis for the blue lines with 1-sigma error bars. The V3FIT reconstruction of the pressure profiles are shown in magenta. The analytic evaluations of the best linear estimate of the 1-σ limits are included as error bars.
Right axis (Transform): The red line is the rotational transform from the V3FIT reconstruction with plasma.

The quality-of-fit metric, g^2, is now shown.

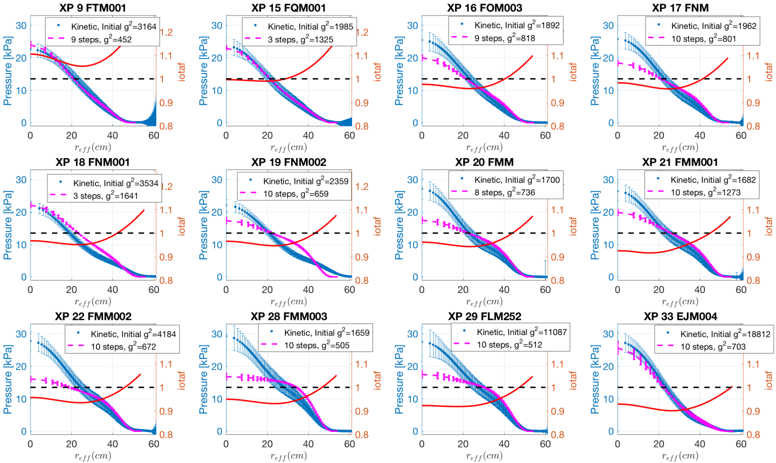

Figure 5: Left axis (Pressure): Kinetic profile data is the basis for the blue lines with 1-sigma error bars. The V3FIT reconstruction of the pressure profiles are shown in magenta. The analytic evaluations of the best linear estimate of the 1-σ limits are included as error bars. Right axis (Transform): The red line is the rotational transform from the V3FIT reconstruction with plasma.

Reconstructions of the total stored energy mostly agree. Pressure profiles only sometimes agree with kinetic profiles.

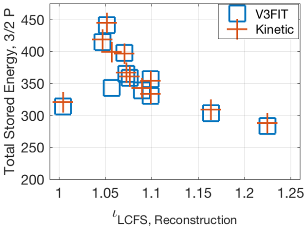

- 5/5-islands may be altering the local current density distribution, causing problems for the magnetics-based equilibrium reconstruction
  - XPs 16 - 29: When the 5/5 islands are in the periphery, $r_{eff}|_{\iota=1} \in [40cm, 50cm]$, the reconstructed profiles differ from those derived from kinetic data (Thomson + XICS)
  - XPs 9, 15, 33: Reconstructed pressure profiles agree with the kinetic profiles when $\iota = 1$ is not in the periphery of the plasma
  - Non-nested MHD solution (SIESTA (easy?), SPEC (hard?))
- Kinetic Profiles
  - Initial guess based on vacuum solution
  - Density was adjusted to match measured diamagnetic energy
  - Finite beta effects may play a role in profile modeling

The bootstrap current + relaxing current profile model (left, middle) qualitatrively agree with the total reconstructed current (right). Residual ECCD and uncertainty in the input profiles may account for the quantitative differences for $t \geq 10$ *sec*.

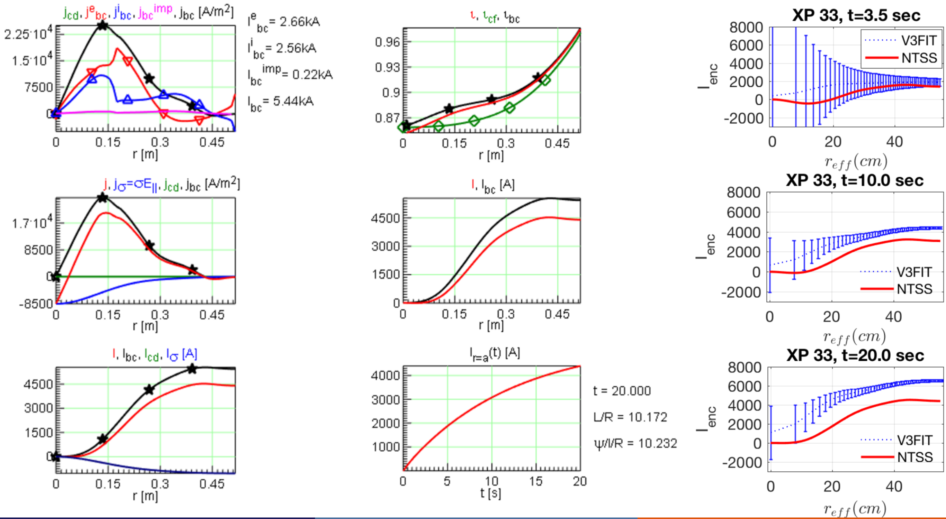

Bootstrap current reconstructions

- Early in time, $t \leq 3.5\ sec$, large uncertainties in reconstructed current profile.
- Later in time, profile shape becomes more certain, although core current density is largely unconstrained.
- Reconstructed current profile shapes with $N_{cssq} = 3$ free regions of toroidal current density agree with bootstrap model.
- Results with $N_{cssq} = 4$ regions have larger uncertainties/too many degrees of freedom.
- Residual ECCD (Up to 1 kA) and uncertainties in the NTSS input profiles for the bootstrap current may account for the observed differences between the model predictions and the reconstructions.
- Local Measurements / Constraints can provide localized 'priors'.
- Spectroscopic 'measurements' of localized current density, or multiple chords of $\int f(B)\, dl$ may help constrain the local current density far from edge.
- Characterization of transient events may require internal measurements.

Next steps for V3FIT reconstructions of current and pressure profiles

- Extend analysis to remaining OP 1.2B bootstrap discharges
- Explore using 'priors' on pressure and current profiles
- Re-visit ECCD discharges
- Islands & Non-nested MHD solutions
    - SIESTA (easy)
    - SPEC (hard)
- Kinetic Profiles
    - Electron and ion profiles in V3FIT are restricted to $T_e \propto T_i$.
- Explore the features that are seen in the data but are not resolved by the reconstructions (Saddle loops and segmented Rogowski coils)
- Explore spectroscopic alternatives for constraining the rotational transform, current, or current density profile